A 3D Model of CYP1B1 Explains the Dominant 4-Hydroxylation of Estradiol

Toshimasa Itoh,[†] Hitomi Takemura,[‡,§] Kayoko Shimoi,[§] and Keiko Yamamoto*,[†]

Laboratory of Drug Design and Medicinal Chemistry, Showa Pharmaceutical University, 3-3165 Higashi-Tamagawagakuen, Machida, Tokyo 194-8543, Japan, Faculty of Human Health Sciences, Matsumoto University, 2095-1 Niimura, Matsumoto 390-1295, Japan, and Institute for Environmental Sciences, University of Shizuoka, 52-1 Yada, Suruga, Shizuoka 422-8526, Japan

Received February 6, 2010

CYP1A1 and CYP1A2 exhibit catalytic activity predominantly for the 2-hydroxylation of estradiol, whereas CYP1B1 exhibits catalytic activity predominantly for 4-hydroxylation of estradiol. To understand why CYP1B1 predominantly hydroxylates the 4-position of estradiol, we constructed three-dimensional structures of CYP1A1 and CYP1B1 by homology modeling, using the crystal structure of CYP1A2, and studied the docking mode of estradiol with CYP1A1, CYP1A2, and CYP1B1. The results demonstrated that two particular amino acid residues for each CYP, namely Thr124 and Phe260 of CYP1A2, Ser122 and Phe258 of CYP1A1, and Ala133 and Asn265 of CYP1B1, play an important role in estradiol recognition.

INTRODUCTION

The endogenous estrogens, 17β-estradiol (E_2) and estrone (E_1), have long been recognized as prime risk factors for the development of breast cancer.[1] It is now known that oxidative estrogen metabolism is a critical factor in the development of human breast cancer.[2,3] Figure 1 shows the metabolic pathway of the main estrogen, E_2, in the mammary gland. Metabolism is regulated by the oxidizing enzymes CYP1A1 and CYP1B1 and by catechol-*O*-methyltransferase (COMT). CYP1A1 exhibits catalytic activity predominantly for the 2-hydroxylation of E_2 to yield 2-hydroxyestradiol (2-OHE_2).[4,5] 2-OHE_2 is rapidly methylated by COMT to produce 2-methoxyestradiol (2-$MeOE_2$), which is known to be noncarcinogenic and to inhibit the proliferation of cancer cells. CYP1B1 exhibits catalytic activity predominantly for the 4-hydroxylation of E_2 to yield 4-hydroxyestradiol (4-OHE_2).[4,5] 4-OHE_2 is mainly oxidized by peroxidases to produce estradiol-3,4-semiquinone (E_2-3,4-SQ) and estradiol-3,4-quinone (E_2-3,4-Q). E_2-3,4-Q forms a quinone−DNA adduct, causing mutations and initiating carcinogenesis. Recently, a quinone metabolite, E_2-3,4-Q, was identified as a potential risk factor in breast cancer.[6]

Liehr and Ricci reported that 4-hydroxylation of E_2 is a marker for human mammary tumors.[7] In the breast, 4-hydroxylation is the dominant metabolic pathway for E_2 because the expression level of CYP1B1 is higher than that of CYP1A1. In addition, CYP1B1 is expressed more highly in breast cancer tissue than in normal breast tissue.[8,9] Consequently, the concentration of 4-OHE_2 in human breast cancer is higher than that in normal tissue.[3] Therefore, a CYP1B1 inhibitor might be promising as a drug for the prevention and treatment of breast cancer. To understand the molecular basis of carcinogenesis induced by E_2, it is important to know why CYP1A1 and CYP1B1 predominantly hydroxylate the C2- and C4-position, respectively, of E_2.

CYP1A2 is the principal family 1 enzyme expressed in the human liver and contributes to the hepatic metabolism of E_2 to produce 2-OHE_2. Recently Sansen et al. reported the X-ray crystal structure of human CYP1A2.[10] In this article, we report the three-dimensional (3D) structures of CYP1A1 and CYP1B1 constructed by homology modeling using the crystal structure of CYP1A2 as a template. We also report results of the docking study of E_2 into CYP1A2, CYP1A1, and CYP1B1 that indicates structural reasons why CYP1A1 and CYP1A2 predominantly hydroxylate the C2-position, whereas CYP1B1 hydroxylates the C4-position of E_2.

MATERIALS AND METHODS

Sequence Alignment. We aligned the three human CYPs responsible for estrogen metabolism, CYP1A1, CYP1B1, and CYP1A2, using the ClustalW2 program (http://www.ebi.ac.uk/Tools/clustalw2/).[11] A part of the computationally derived alignment was modified manually (see the Results Section).

Modeling. Based on the alignment, we constructed a 3D model of CYP1B1 and CYP1A1 by sequence replacement using the SYBYL Biopolymer program[12] (Tripos Inc.) and the atomic coordinates (Arg34−Ser513) of the crystal structure of CYP1A2 (PDB; 2HI4) as a template.[10] The procedure was as follows: First of all, the structure of residues in the structurally conserved regions, consisting of helices, β-strands, and loops with the same number of amino acid residues as the template, was constructed. Side chain conformational angles in the residues are retained as far as possible. The positions of the hydrogens added are determined by data in SYBYL's internal tables for bond lengths and angles. Second, other parts of the CYP structure were constructed manually using the Coot 0.5.2 program[13] by applying torsion and Ramachandran restraints. Then, heme

* Corresponding author. Telephone: +81 42 721 1580. Fax: +81 42 721 1580. E-mail: yamamoto@ac.shoyaku.ac.jp.
[†] Showa Pharmaceutical University.
[‡] Matsumoto University.
[§] University of Shizuoka.

10.1021/ci1000554 © 2010 American Chemical Society
Published on Web 05/12/2010

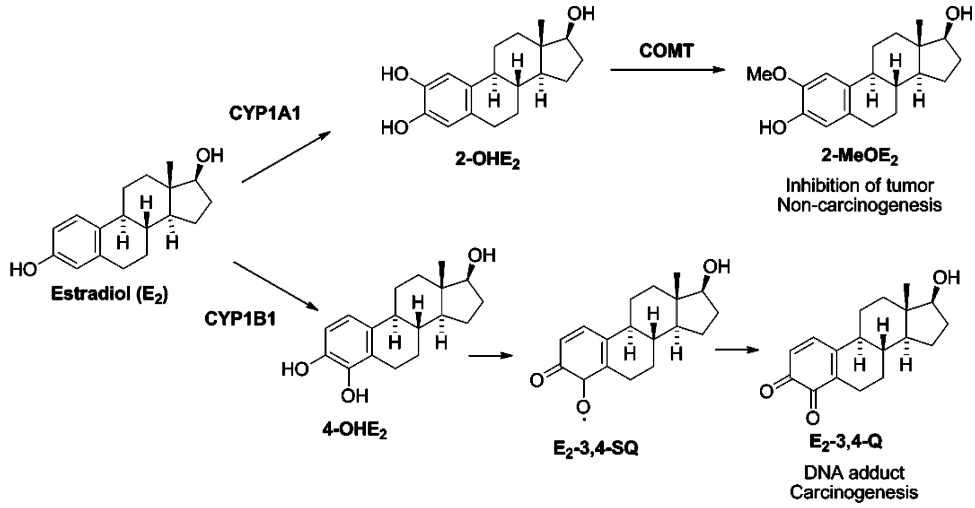

Figure 1. Metabolic pathways of estradiol (E_2) catalyzed by CYP1A1 and CYP1B1 in the breast. The metabolism is regulated by oxidizing enzymes, CYP1A1 and CYP1B1, and catechol-*O*-methyltransferase (COMT). CYP1A1 exhibits catalytic activity dominantly for the 2-hydroxylation of E_2 to afford 2-hydroxyestradiol (2-OHE_2). 2-OHE_2 is rapidly methylated by COMT to produce 2-methoxyestradiol (2-$MeOE_2$). CYP1B1 exhibits the catalytic activity dominantly for the 4-hydroxylation of E_2 to afford 4-hydroxyestradiol (4-OHE_2). 4-OHE_2 is mainly oxidized by peroxidases to produce estradiol-3,4-semiquinone (E_2-3,4-SQ) and estradiol-3,4-quinone (E_2-3,4-Q).

was merged into the protein to occupy the same position as the heme of the template protein, CYP1A2. Finally, energy minimization of the constructed structure was performed until the energy gradient was lower than 0.1 kcal/(mol Å) using the Tripos force field. The validity of the CYP1A1 and CYP1B1 models was evaluated using PROCHECK in the CCP4 program.[14]

Docking. Docking was performed using Surflex Dock in Sybyl 8.0 (Tripos). The crystal structure of CYP1A2 (PDB: 2HI4) and the CYP1A1 and CYP1B1 models constructed above were used as the CYP protein structure. Surflex Dock[15] program uses an empirical scoring function (based on the Hammerhead docking system) that has been updated and reparameterized with additional negative training data,[16] along with a search engine that relies on a surface-based molecular similarity method.[17,18] We applied the "hard grid treatment" method in which side chains of the active site residues are fixed, because we considered that flexibility of those side chains is minimum judging from the clear electron density map and the low B-factors of the CYP1A2 crystal structure. More than 40 substrate structures were obtained for each CYP. Substrate structures with the top 20 scores were selected, and then structures whose A-ring was positioned within 5.5 Å[19] from the heme iron atom in CYP were extracted. Energy minimization (Tripos force field) of each substrate−CYP complex was performed to give the final complex model.

RESULTS AND DISCUSSION

Sequence Alignment. Figure 2 shows the final alignment of the CYP1A1, CYP1A2, and CYP1B1 sequences. A part of the computationally derived alignment was modified manually. Campos−Mollo reported that the F261L mutation in CYP1B1 causes primary congenital glaucoma (PCG) without affecting the stability of the CYP,[20] suggesting that F261 is a critical residue for expression of the function. We thought that F261 faces the surface of the active site of CYP1B1. Therefore, we manually modified the computationally derived alignment to align F261 of CYP1B1 with F256 of CYP1A2.

Compared with template CYP1A2, CYP1B1 has four deletion and two insertion segments, and CYP1A1 has one deletion and one insertion segment. Sequence identity of CYP1A1 with CYP1A2 is 72%, whereas that of CYP1B1 with CYP1A2 is 37%. Highly conserved and functionally important residues in the CYP superfamily are: (1) three absolutely conserved residues, ExxR in the K helix and Cys just before the L helix (for example E387, R390, and C470 in CYP1B1); (2) the consensus sequence (A/G)(G/S)x(E/D)T in the center of the I helix; and (3) the consensus sequence F(G/S)xGx(H/R)xCxGxx(I/L/F)(A/S) containing the Cys (C470 in CYP1B1) responsible for heme binding.[21,22] As shown in Figure 2, these important segments of the three CYP sequences correctly align with each other. In addition, the segments of the CYP1B1 and CYP1A1 sequences corresponding to the secondary structure elements of the CYP1A2 crystal structure do not have any gaps or insertions (Figure 2), indicating that most of the secondary structure is conserved.

Modeling. The constructed 3D models of CYP1A1 and CYP1B1 are shown in Figure 3. The N-terminal regions of CYP1A1 (Met1−Pro31) and CYP1B1 (Met1−Gln42) were not constructed because the coordinates of the corresponding region of CYP1A2 (Met1−Pro33) were not determined. We evaluated the model structure by using the PROCHECK in the CCP4 program. A Ramachandran plot showed that 99.1% of the residues in CYP1A1 and 98.1% of the residues in CYP1B1 are in either the most favored or allowed regions.

The 3D structures of CYP1A1 and CYP1B1 were similar to those of other CYPs reported to date.[10,23−32] The structures contain 12 α-helices and 4 β-sheets and have several additional helices, as does the template CYP1A2. In our models, Glu(E)374, Arg(R)377, and Arg(R)431 of CYP1A1 (Figure 3b) and Glu(E)387 and Arg(R)390 and Arg(R)444 of CYP1B1 (Figure 3c) form the ERR triad that is the conserved folding core in the CYP1 family. In the CYP1B1 model, Ala330 and Thr334 in helix I are highly conserved; the hydroxyl group of the Thr334 side chain forms a hydrogen bond with the backbone carbonyl oxygen of Ala330. Thr334, which is located near the heme, is thought

```
1B1    1 MGTSLSPNDP WPLNPLSIQQ TTLLLLLSVL ATVHVGQRLL RQRRRQLRSA PPGPFAWPLI GNAAAVGQAA HLSFARLARR  80
1A1    1 ---------- -MLFPISMSA TEFLLASVIF CLVFWVIRAS RPQVPKGLKN PPGPWGWPLI GHMLTLGKNP HLALSRMSQQ  69
1A2    1 ---------M ALSQSVPFSA TELLLASAIF CLVFWVLKGL RPRVPKGLKS PPEPWGWPLL GHVLTLGKNP HLALSRMSQR  71
                     .:.:.  * :**   :: . *.   :    * :  :  .  ** *:.***: *:  ::*: . **:::*::::
                                                                                         A

                                                          SRS1
1B1   81 YGDVFQIRLG SCPIVVLNGE RAIHQALVQQ GSAFADRPAF ASFRVVSGGR SMAFGHYS-E HWKVQRRAAH SMMRNF-FTR 158
1A1   70 YGDVLQIRIG STPVVVLSGL DTIRQALVRQ GDDFKGRPDL YTFTLISNGQ SMSFSPDSGP VWAARRRLAQ NGLKSFSIAS 149
1A2   72 YGDVLQIRIG STPVLVLSRL DTIRQALVRQ GDDFKGRPDL YTSTLITDGQ SLTFSTDSGP VWAARRRLAQ NALNTFSIAS 151
         ****:***:* * *::**.      :*:****:* *. * .** :  : :::.*: *::*.   *     * .:** *: . :..* ::
                        B                    B′                     C

                                                                                     SRS2
1B1  159 QPRSRQ--VL EGHVLSEARE LVALLVRGSA DGAFLDPRPL TVVAVANVMS AVCFGCRYSH DDPEFRELLS HNEEFGRTVG 236
1A1  150 DPASSTSCYL EEHVSKEAEV LISTLQELMA GPGHFNPYRY VVVSVTNVIC AICFGRRYDH NHQELLSLVN LNNNFGEVVG 229
1A2  152 DPASSSSCYL EEHVSKEAKA LISRLQELMA GPGHFDPYNQ VVVSVANVIG AMCFGQHFPE SSDEMLSLVK NTHEFVETAS 231
          :* *      * * ** .**.   *:: *  .   *  . ..::*    .**:*:**:  *:*** :: .  .  *: .*:.   ..:* ....
                        D                     E                F      F

                      SRS3
1B1  237 AGSLVDVMPW LQYFPNPVRT VFREFEQLNR NFSNFILDKF LRHCESLRPG AAPRDMMDAF ILSAEKKAAG DSHGGARLD 316
1A1  230 SGNPADFIPI LRYLPNPSLN AFKDLNEKFY SFMQKMVKEH YKTFEKGH-- I--RDITDSL IEHCQEKQL- -DENANVQLS 303
1A2  232 SGNPLDFFPI LRYLPNPALQ RFKAFNQRFL WFLQKTVQEH YQDFDKNS-- V--RDITGAL FKHSKKGP-- --RASGNLIP 303
         :*.  *.:*  *:*:***    *: ::     * :  :.:.  :  :.:       **: .:: :  .::        ..  :
           F′    G′          G                        H

         SRS4                                                                            SR
1B1  317 LENVPATITD IFGASQDTLS TALQWLLLLF TRYPDVQTRV QAELDQVVGR DRLPCMGDQP NLPYVLAFLY EAMRFSSFVP 396
1A1  304 DEKIINIVLD LFGAGFDTVT TAISWSLMYL VMNPRVQRKI QEELDTVIGR SRRPRLSDRS HLPYMEAFIL ETFRHSSFVP 383
1A2  304 QEKIVNLVND IFGAGFDTVT TAISWSLMYL VTKPEIQRKI QKELDTVIGR ERRPRLSDRP QLPYLEAFIL ETFRHSSFLP 383
          *::   : * :***. **::  **::* *: :  .   * :* :: * *** *:** .* * :.*:. :***: **:  *::*.***:*
                 I                     J                            K

S5
1B1  397 VTIPHATTAN TSVLGYHIPK DTVVFVNQWS VNHDPVKWPN PENFDPARFL DKDG-LINKD LTSRVMIFSV GKRRCIGEEL 475
1A1  384 FTIPHSTTRD TSLKGFYIPK GRCVFVNQWQ INHDQKLWVN PSEFLPERFL TPDG-AIDKV LSEKVIIFGM GKRKCIGETI 462
1A2  384 FTIPHSTTRD TTLNGFYIPK KCCVFVNQWQ VNHDPELWED PSEFRPERFL TADGTAINKP LSEKMMLFGM GKRRCIGEVL 463
         .****:** :  *:: *::***    ******. :***      * : *.:* * ***    **  *:*  *:.::::*.: ***:**** :

                                          SRS6
1B1  476 SKMQLFLFIS ILAHQCDFRA NPNEPAKMNF SYGLTIK-PK SFKVNVTLRE SMELLDSAVQ NLQAKETCQ  543
1A1  463 ARWEVFLFLA ILLQRVEFSV PLGVKVDMTP IYGLTMKHAC CEHFQMQLRS ---------- ---------  512
1A2  464 AKWEIFLFLA ILLQQLEFSV PPGVKVDLTP IYGLTMKHAR CEHVQARLRF SIN------- ---------  516
         :: ::***:: ** :: :* .    .   ..:.    ****:* .   . .:.   **
          L

▮ Substrate binding cavity in 2HI4.pdb
▬ alpha helix    ▬ beta sheet
```

Figure 2. Sequence alignment of CYP1B1 and CYP1A1 with CYP1A2. The A−L helices are noted below the CYP1A2 sequence based on its crystal structure. β-Sheets are indicated with green bars. Blue boxes represent substrate recognition sites 1−6 (SRS1-6). In the crystal structure of CYP1A2, residues whose side chain faces the substrate-binding pocket surface are shown with yellow boxes.

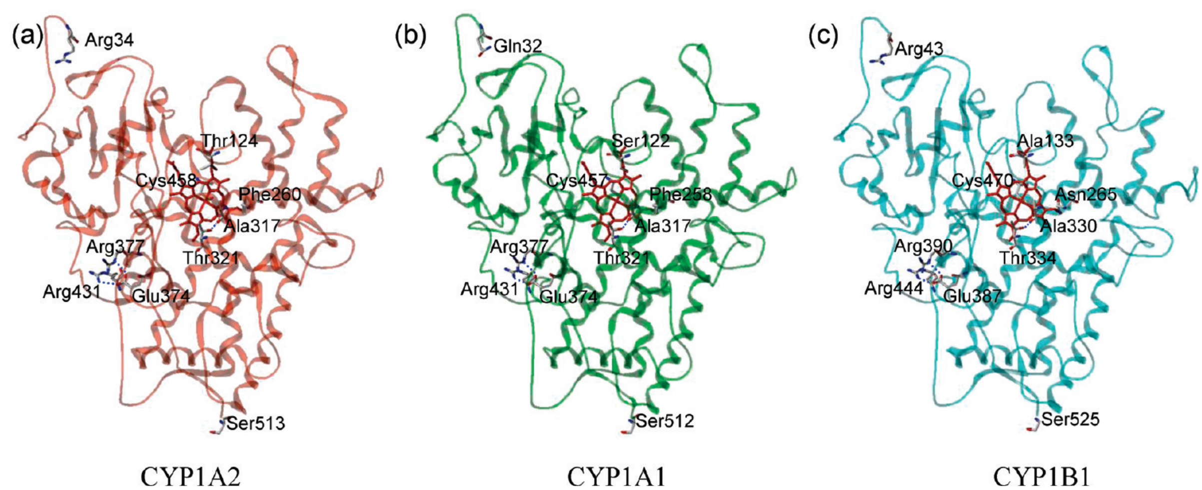

Figure 3. Three-dimensional structures of CYP1A2, CYP1A1, and CYP1B1. Heme is shown as a red stick representation. The ERR triad is shown on the left side of each structure. Hydrogen bonds are presented as dotted blue lines.

to be involved in the oxygen activation mechanism.[19] The same structure is observed in the CYP1A1 model.

Figure 4 shows the structure of the active site pocket of the three CYPs and the residues whose side chain faces the

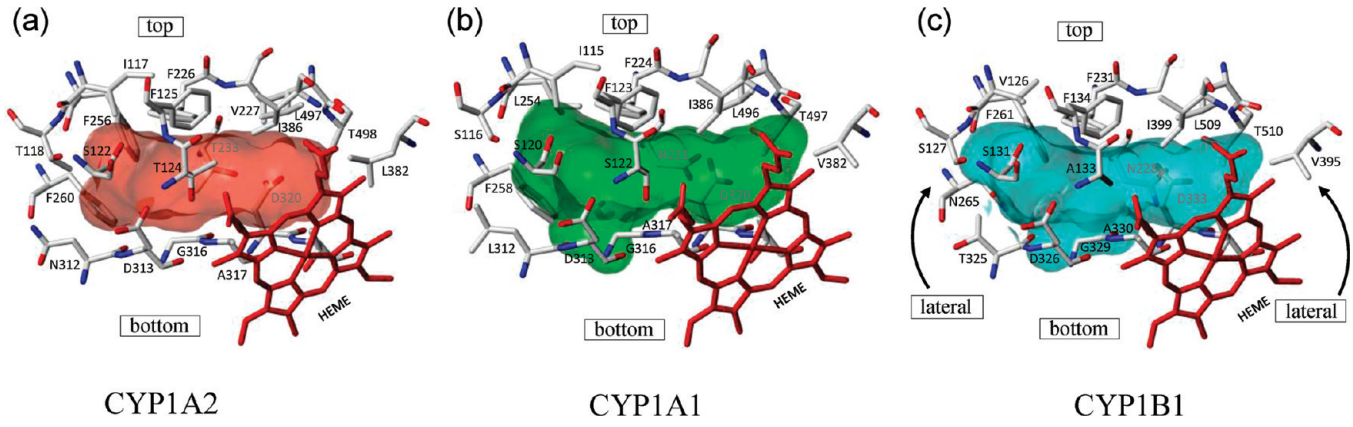

Figure 4. The structure of the active site pocket of the three CYPs and the residues whose side chain faces the pocket surface. The three CYPs have a closed and planar pocket lacking a water or substrate access channel. Residues at the top or the bottom are highly conserved, while residues at the lateral part are variable, for example, Thr124, Phe260, and Asn312 of CYP1A2, Ser122, Phe258, and Leu312 of CYP1A1, and Ala133, Asn265, and Thr325 of CYP1B1.

pocket surface. The three CYPs have a closed and planar pocket lacking a water or substrate access channel (Figure 4a−c). The substrates for these three CYPs have a planar structure, thus, this planar pocket is consistent with the common structural feature of the substrates. The volumes of the CYP1A1 and CYP1B1 active sites are 600 and 550 Å^3, respectively, which are larger than that of CYP1A2 (470 Å^3). It should be noted that all residues whose side chain faces the substrate-binding pocket are located at the six substrate-recognition sites (SRS) proposed by Gotoh[33] (Figures 2 and 4). The identities of those residues between CYP1B1 and CYP1A1, CYP1B1 and CYP1A2, and CYP1A1 and CYP1A2 are 74, 63, and 68%, respectively. As shown in Figure 4, residues whose side chain faces the top or bottom of the substrate-binding pocket are highly conserved. In contrast, residues whose side chain faces a lateral part of the substrate-binding pocket are variable. These results imply that nonconserved residues at lateral positions, such as Thr124, Phe260, and Asn312 of CYP1A2, Ser122, Phe258, and Leu312 of CYP1A1, and Ala133, Asn265, and Thr325 of CYP1B1, play an important role in substrate recognition.

Docking. We obtained more than 40 E_2−CYP complex structures for each CYP, from which we selected the E_2 conformers with the top 20 scores because they covered all the representative conformations of E_2. Figures 5a−c show the 20 conformations of E_2 for each CYP. We found that there are five binding modes toward CYP1A2 and CYP1A1 (Figure 5a and b) and nine modes toward CYP1B1 (Figure 5c). These representative five binding modes toward CYP1A2 and CYP1A1 and the nine binding modes toward CYP1B1 are designated in Figure 5a−c as five and nine blue arrows, respectively, which point to the oxygen of the 3-hydroxyl group of E_2. To investigate the positional selectivity of hydroxylation at the A-ring, we chose conformers having an A-ring carbon within 5.5 Å of the heme Fe atom.[19] These conformers were thought to be adequate representations of the structure prior to oxidation at the A-ring. Two binding modes were found in CYP1B1 (Figure 5f and i), while only one binding mode was found in CYP1A2 and CYP1A1 (Figure 5d and e). To distinguish the two types of binding modes, we termed the complexes shown in Figure 5d−f and i "methyl up" and "methyl down" complexes, respectively, based on the direction of the 18-methyl group of E_2.

In each "methyl up" complex, appropriate hydrophobic interactions between E_2 and the CYP were observed, but no hydrogen bonds were apparent (Figure 5d−f). Interestingly, in the "methyl down" complex (Figure 5i), a hydrogen bond between the 17-hydroxyl group of E_2 and Asn265 of CYP1B1 was observed in addition to hydrophobic interactions. Docking analysis was performed to better understand why E_2 cannot adopt a "methyl down" conformer in CYP1A2 and CYP1A1. E_2 was extracted from the "methyl down" complex of CYP1B1 and E_2 (Figure 5i) and merged into CYP1A2 and CYP1A1 (Figure 5g and h). These superimpositions indicated that Thr124 and Phe260 of CYP1A2 and Ser122 and Phe258 of CYP1A1 are sufficiently close (less than 3.2 Å) to cause steric clash with the B-ring and the 17-hydroxyl group of the substrate (Figure 5g and h). These results indicate that Thr124 and Phe260 of CYP1A2, Ser122 and Phe258 of CYP1A1, and Ala133 and Asn265 of CYP1B1 are critical residues for E_2 recognition.

Several papers concerning the importance of various residues for CYP1A activity were reported.[34–38] Guengerich's group generated random libraries of human CYP1A2 with substrate-recognition sequences mutated and obtained mutants that alter the intervening steps leading to the formation of the activated Michaelis complex.[34,35] Szklarz's group performed modeling and mutation studies of CYP1A1 and indicated the importance of Val382 for recognition of the side chain of resorufin derivatives.[36] In addition, Thr124 of CYP1A2 and Ser122 of CYP1A1 were demonstrated to play an important role for alkoxyresorufin metabolism.[37] This demonstration is in agreement with our suggestion that Thr124 of CYP1A2, Ser122 of CYP1A1, and Ala133 of CYP1B1 are important residues for substrate recognition.

It is clear that the "methyl up" conformations are oxidized at the C2-position (Figure 5d−f), whereas the "methyl down" conformations are oxidized at the C4-position (Figure 5i). The docking study suggests that CYP1A2 and CYP1A1 preferentially generate 2-OHE_2 rather than 4-OHE_2 and that CYP1B1 generates both 2-OHE_2 and 4-OHE_2. This suggestion is supported by a report from Lee et al. that CYP1A1 and CYP1A2 produce 2-OHE_2 and 4-OHE_2 in a ratio of >10:1, whereas CYP1B1 produces 2-OHE_2 and 4-OHE_2 in a ratio of 1:3.[39] Preference for 4-hydroxylation by CYP1B1 can be explained by the hydrogen bond between the 17-hydroxyl

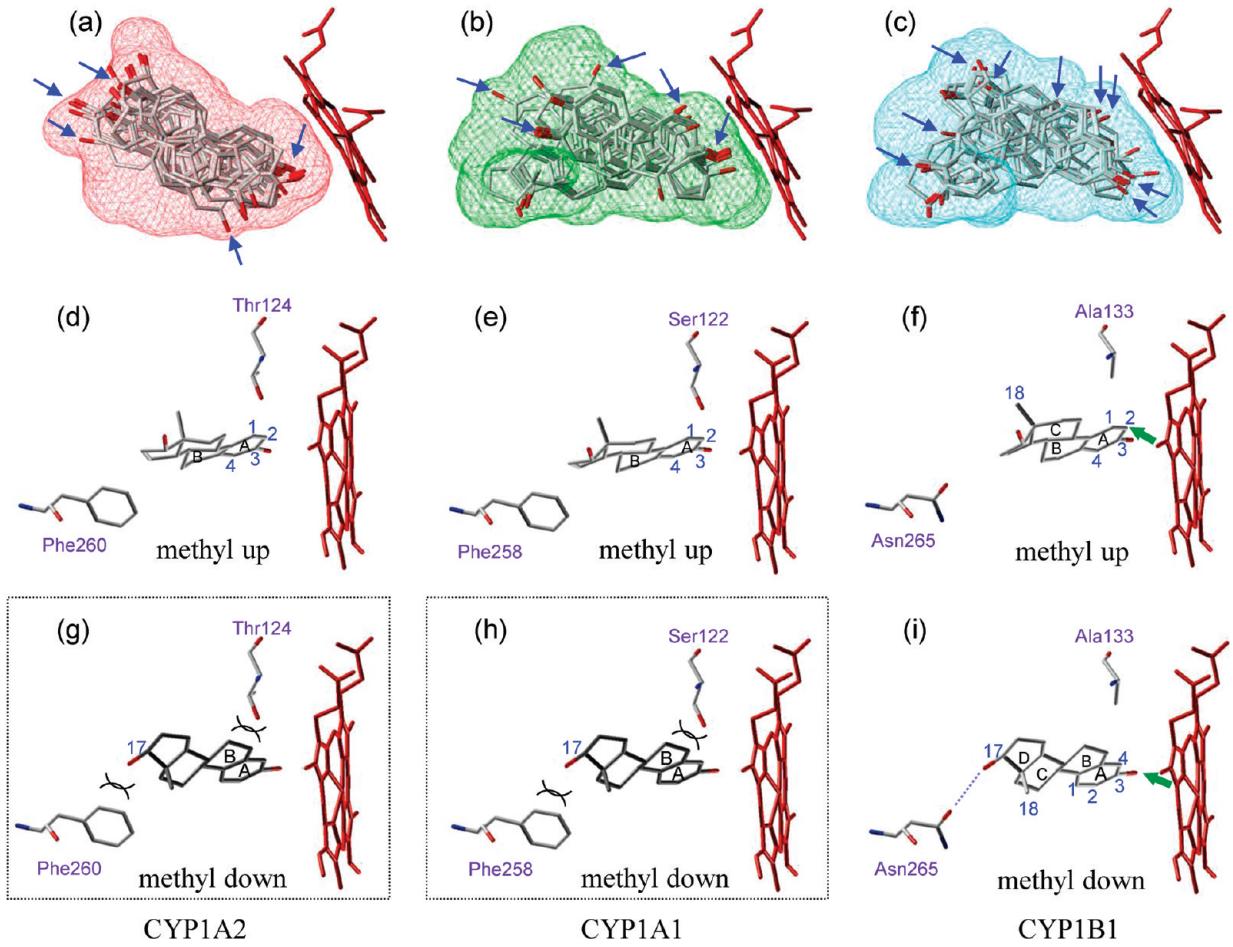

Figure 5. Docking structures of E_2 into CYP1A2, CYP1A1, and CYP1B1. E_2 and amino acid residues are presented as stick models in atom type. Heme is shown as stick model in red. E_2 conformers with top 20 scores are presented (a−c). Red (a), green (b), and cyan (c) lines represent the Connolly channel surface of the substrate-binding pocket of CYP1A2, CYP1A1, and CYP1B1, respectively. Representative binding modes are shown by representing the 3-hydroxyl group of E_2 with five (a and b) and nine (c) blue arrows. "Methyl up" complex of E_2 and CYP1A2 (d), CYP1A1 (e), and CYP1B1 (f) and "methyl down" complex of E_2 and CYP1B1 (i). Superimposition of "methyl down" conformer of E_2 and CYP1A2 (g) and CYP1A1 (h).

group and Asn265; only the "methyl down" conformer forms this favorable hydrogen bond in CYP1B1. Thus, our docking model is consistent with the specific 4-hydroxylation of E_2.

Lee et al. reported that the rank order of the reaction rate for E_2 is 1A2 > 1A1≫ 1B1. We suggest that one of the reasons for this order is the entropic advantages of CYP1A2 and CYP1A1.[39] Since the shape of the CYP1B1 substrate-binding pocket is rounder than those of CYP1A2 and CYP1A1, as shown in Figure 5a−c, CYP1B1 allows multiple conformations of E_2 to be accommodated. This is consistent with the docking simulation results described above, in which nine binding modes appeared in CYP1B1 but only five binding modes appeared in CYP1A2 and CYP1A1.

CONCLUSIONS

The preference for 2-hydroxylation of E_2 by CYP1A2 and CYP1A1 was investigated by docking analysis of E_2, and the analysis suggested that only the "methyl up" complex is allowed. The analysis also suggested that the preference for 4-hydroxylation of E_2 by CYP1B1 is due to both "methyl up" and "down" complexes being acceptable but with "methyl down" being preferred due to the presence of a hydrogen bond between E_2 and CYP. Furthermore, Thr124 and Phe260 of CYP1A2, Ser122 and Phe258 of CYP1A1, and Ala133 and Asn265 of CYP1B1 were indicated to be critical residues for E_2 recognition.

REFERENCES AND NOTES

(1) Pike, M. C.; Krailo, M. D.; Henderson, B. E.; Casagrande, J. T.; Hoel, D. G. 'Hormonal' risk factors, 'breast tissue age' and the age-incidence of breast cancer. *Nature* **1983**, *303*, 767–770.
(2) Rogan, E. G.; Badawi, A. F.; Devanesan, P. D.; Meza, J. L.; Edney, J. A.; West, W. W.; Higginbotham, S. M.; Cavalieri, E. L. Relative imbalances in estrogen metabolism and conjugation in breast tissue of women with carcinoma: potential biomarkers of susceptibility to cancer. *Carcinogenesis* **2003**, *24*, 697–702.
(3) Castagnetta, L. A.; Granata, O. M.; Traina, A.; Ravazzolo, B.; Amoroso, M.; Miele, M.; Bellavia, V.; Agostara, B.; Carruba, G. Tissue content of hydroxyestrogens in relation to survival of breast cancer patients. *Clin. Cancer Res.* **2002**, *8*, 3146–3155.
(4) Zhu, B. T.; Lee, A. J. NADPH-dependent metabolism of 17beta-estradiol and estrone to polar and nonpolar metabolites by human tissues and cytochrome P450 isoforms. *Steroids* **2005**, *70*, 225–244.
(5) Tsuchiya, Y.; Nakajima, M.; Yokoi, T. Cytochrome P450-mediated metabolism of estrogens and its regulation in human. *Cancer Lett.* **2005**, *227*, 115–124.
(6) Parl, F. F.; Dawling, S.; Roodi, N.; Crooke, P. S. Estrogen metabolism and breast cancer: a risk model. *Ann. N. Y. Acad. Sci.* **2009**, *1155*, 68–75.
(7) Liehr, J. G.; Ricci, M. J. 4-Hydroxylation of estrogens as marker of human mammary tumors. *Proc. Natl. Acad. Sci. U.S.A.* **1996**, *93*, 3294–3296.
(8) Spink, D. C.; Spink, B. C.; Cao, J. Q.; DePasquale, J. A.; Pentecost, B. T.; Fasco, M. J.; Li, Y.; Sutter, T. R. Differential expression of CYP1A1 and CYP1B1 in human breast epithelial cells and breast tumor cells. *Carcinogenesis* **1998**, *19*, 291–298.

(9) Murray, G. I.; Taylor, M. C.; McFadyen, M. C.; McKay, J. A.; Greenlee, W. F.; Burke, M. D.; Melvin, W. T. Tumor-specific expression of cytochrome P450 CYP1B1. *Cancer Res.* **1997**, *57*, 3026–3031.
(10) Sansen, S.; Yano, J. K.; Reynald, R. L.; Schoch, G. A.; Griffin, K. J.; Stout, C. D.; Johnson, E. F. Adaptations for the oxidation of polycyclic aromatic hydrocarbons exhibited by the structure of human P450 1A2. *J. Biol. Chem.* **2007**, *282*, 14348–14355.
(11) Li, K. B. ClustalW-MPI: ClustalW analysis using distributed and parallel computing. *Bioinformatics* **2003**, *19*, 1585–1586.
(12) SYBYL Molecular Modeling Software, version 8.0; Tripos Inc.: 1699 South Hanley Road, St. Louis, MO 63144−2913.
(13) Emsley, P.; Cowtan, K. Coot: model-building tools for molecular graphics. *Acta Crystallogr., Sect. D: Biol. Crystallogr.* **2004**, *60*, 2126–2132.
(14) The CCP4 suite: programs for protein crystallography. *Acta Crystallogr., Sect. D: Biol. Crystallogr.* **1994**, *50*, 760−763.
(15) Ruppert, J.; Welch, W.; Jain, A. N. Automatic identification and representation of protein binding sites for molecular docking. *Protein Sci.* **1997**, *6*, 524–533.
(16) Pham, T. A.; Jain, A. N. Parameter estimation for scoring protein-ligand interactions using negative training data. *J. Med. Chem.* **2006**, *49*, 5856–5868.
(17) United States Patent No. 6,470,305; 20.
(18) Jain, A. N. Morphological similarity: a 3D molecular similarity method correlated with protein-ligand recognition. *J. Comput.-Aided Mol. Des.* **2000**, *14*, 199–213.
(19) Sykes, M. J.; McKinnon, R. A.; Miners, J. O. Prediction of metabolism by cytochrome P450 2C9: alignment and docking studies of a validated database of substrates. *J. Med. Chem.* **2008**, *51*, 780–791.
(20) Campos-Mollo, E.; Lopez-Garrido, M. P.; Blanco-Marchite, C.; Garcia-Feijoo, J.; Peralta, J.; Belmonte-Martinez, J.; Ayuso, C.; Escribano, J. CYP1B1 mutations in Spanish patients with primary congenital glaucoma: phenotypic and functional variability. *Mol. Vis.* **2009**, *15*, 417–431.
(21) Graham-Lorence, S. E.; Peterson, J. A. Structural alignments of P450s and extrapolations to the unknown. *Methods Enzymol.* **1996**, *272*, 315–326.
(22) Yamamoto, K.; Masuno, H.; Sawada, N.; Sakaki, T.; Inouye, K.; Ishiguro, M.; Yamada, S. Homology modeling of human 25-hydroxyvitamin D3 1α-hydroxylase (CYP27B1) based on the crystal structure of rabbit CYP2C5. *J. Steroid Biochem. Mol. Biol* **2004**, *89−90*, 167–171.
(23) Zhao, Y.; White, M. A.; Muralidhara, B. K.; Sun, L.; Halpert, J. R.; Stout, C. D. Structure of microsomal cytochrome P450 2B4 complexed with the antifungal drug bifonazole: insight into P450 conformational plasticity and membrane interaction. *J. Biol. Chem.* **2006**, *281*, 5973–5981.
(24) Yano, J. K.; Hsu, M. H.; Griffin, K. J.; Stout, C. D.; Johnson, E. F. Structures of human microsomal cytochrome P450 2A6 complexed with coumarin and methoxsalen. *Nat. Struct. Mol. Biol.* **2005**, *12*, 822–823.
(25) Schoch, G. A.; Yano, J. K.; Sansen, S.; Dansette, P. M.; Stout, C. D.; Johnson, E. F. Determinants of cytochrome P450 2C8 substrate binding: structures of complexes with montelukast, troglitazone, felodipine, and 9-cis-retinoic acid. *J. Biol. Chem.* **2008**, *283*, 17227–17237.
(26) Porubsky, P. R.; Meneely, K. M.; Scott, E. E. Structures of human cytochrome P-450 2E1. Insights into the binding of inhibitors and both small molecular weight and fatty acid substrates. *J. Biol. Chem.* **2008**, *283*, 33698–33707.
(27) Strushkevich, N.; Usanov, S. A.; Plotnikov, A. N.; Jones, G.; Park, H. W. Structural analysis of CYP2R1 in complex with vitamin D3. *J. Mol. Biol.* **2008**, *380*, 95–106.
(28) Wester, M. R.; Johnson, E. F.; Marques-Soares, C.; Dijols, S.; Dansette, P. M.; Mansuy, D.; Stout, C. D. Structure of mammalian cytochrome P450 2C5 complexed with diclofenac at 2.1 A resolution: evidence for an induced fit model of substrate binding. *Biochemistry* **2003**, *42*, 9335–9345.
(29) Rowland, P.; Blaney, F. E.; Smyth, M. G.; Jones, J. J.; Leydon, V. R.; Oxbrow, A. K.; Lewis, C. J.; Tennant, M. G.; Modi, S.; Eggleston, D. S.; Chenery, R. J.; Bridges, A. M. Crystal structure of human cytochrome P450 2D6. *J. Biol. Chem.* **2006**, *281*, 7614–7622.
(30) Williams, P. A.; Cosme, J.; Vinkovic, D. M.; Ward, A.; Angove, H. C.; Day, P. J.; Vonrhein, C.; Tickle, I. J.; Jhoti, H. Crystal structures of human cytochrome P450 3A4 bound to metyrapone and progesterone. *Science* **2004**, *305*, 683–686.
(31) Williams, P. A.; Cosme, J.; Ward, A.; Angove, H. C.; Matak Vinkovic, D.; Jhoti, H. Crystal structure of human cytochrome P450 2C9 with bound warfarin. *Nature* **2003**, *424*, 464–468.
(32) Mestres, J. Structure conservation in cytochromes P450. *Proteins* **2005**, *58*, 596–609.
(33) Gotoh, O. Substrate recognition sites in cytochrome P450 family 2 (CYP2) proteins inferred from comparative analyses of amino acid and coding nucleotide sequences. *J. Biol. Chem.* **1992**, *267*, 83–90.
(34) Parikh, A.; Josephy, P. D.; Guengerich, F. P. Selection and characterization of human cytochrome P450 1A2 mutants with altered catalytic properties. *Biochemistry* **1999**, *38*, 5283–5289.
(35) Yun, C. H.; Miller, G. P.; Guengerich, F. P. Rate-determining steps in phenacetin oxidations by human cytochrome P450 1A2 and selected mutants. *Biochemistry* **2000**, *39*, 11319–11329.
(36) Liu, J.; Ericksen, S. S.; Besspiata, D.; Fisher, C. W.; Szklarz, G. D. Characterization of substrate binding to cytochrome P450 1A1 using molecular modeling and kinetic analyses: case of residue 382. *Drug. Metab. Dispos.* **2003**, *31*, 412–420.
(37) Liu, J.; Ericksen, S. S.; Sivaneri, M.; Besspiata, D.; Fisher, C. W.; Szklarz, G. D. The effect of reciprocal active site mutations in human cytochromes P450 1A1 and 1A2 on alkoxyresorufin metabolism. *Arch. Biochem. Biophys.* **2004**, *424*, 33–43.
(38) Zhou, S. F.; Yang, L. P.; Wei, M. Q.; Duan, W.; Chan, E. Insights into the Structure, Function, and Regulation of Human Cytochrome P450 1A2. *Curr. Drug Metab.* **2009**, *10*, 713–729.
(39) Lee, A. J.; Cai, M. X.; Thomas, P. E.; Conney, A. H.; Zhu, B. T. Characterization of the oxidative metabolites of 17beta-estradiol and estrone formed by 15 selectively expressed human cytochrome p450 isoforms. *Endocrinology* **2003**, *144*, 3382–3398.

CI1000554